FSI Analysis of Upset Loads Due to Material Build Up In Raked Thickeners

Yaojun Lu, Thien Sok, Fred Schoenbrunn, Jeremy Scott, and Craig Gilbert

FLSmidth, Midvale, Utah, USA, 84047

Introduction

The raked thickener is a primary piece of equipment in the mineral processing industry, where a raking mechanism plays a crucial role for smooth thickening operation. The thickener rake basically performs two functions: (1) to scrape and transport mud-bed material to underflow, (2) to enhance dewatering of thickened sediment. It is therefore essential to realistically quantify the rake loads for a reliable rake design so that the underflow with expected density can be produced to meet process specifications.

Although the rake system is a critical part in gravity thickeners, the detailed raking process is poorly understood to date. The existing studies are focused more on clarifiers for wastewater treatment (Warden 1981, Gunthert 1984, Albertson, 1992, Frost 1993) and fundamental investigation on down-scaled lab or pilot thickeners for mineral processing (Rudman 2008, Rudman 2010, Sutalo 2003). Due to significant difference in working fluids, discrepancy in configuration and process conditions, as well as scale-up effect involved, it is questionable to apply these research outcomes to design of a full-scale industry thickener for field applications. In practice, the rake design and operation rely heavily on the best engineering experience that are largely qualitative in nature. For instance, as a key design factor for sizing the rake mechanism and capacity of the driving system, it is still a challenge to predict the rake load over its service life. So far, the rake loads are mainly estimated based on empirical correlation, bench-top test, or small-scale raked cylinder test. Such an empirical-based approach could come up either overestimated or underestimated rake loads, which could lead to a poor rake design, and further contribute to the ratholing, material build up, rake-blockage, and insufficient underflow density during field operation.

To advance the rake design and operation, a FSI (Fluid Structure Interaction) approach has been developed for numerical prediction of the rake loads in an industry thickener under normal operating condition (Lu, et al 2024), which accounts for the all mud-rake interaction in a full-sized thickener operated in field conditions. As an extended study, this paper tries to extend such an FSI approach for quantification of the upset loads at exceptional conditions, where significant thick materials are accumulated in a region of the floor bed to mimic the field observations. Moreover, two materials build-up scenarios were investigated, followed by detailed FSI analysis, in which the CFD (Computational Fluid Dynamics) simulation is carried out to capture the associated hydraulic loads, and the CFD solution is then mapped into an FEA (Finite Element Analysis) solver for strength analysis. Due to the seamless load transition from CFD to FEA solvers, more realistic rake loads can be predicted, which incorporate the full feed conditions, slurry rheology, mud-bed profile, rake configuration, etc., and a more reliable rake design can be obtained. Such a high-fidelity approach can be applied for sizing a new thickener or troubleshooting an existing thickener.

Rake Loads

For mineral processing applications, the thickener rake is either suspended from a bridge or supported on a central support column and driven by a central or a peripheral driving system to deliver high torque, low speed outputs. Even though electronic sensors are applied to monitor and control the rake torque and to prevent damage due to overload, numerous operational incidents have been reported in field operation, including torque spikes, ratholing, rake blockage, variable underflow density, etc. It is therefore essential to realistically quantify the rake loads for a more effective design of the rake system. From an operational perspective, the rake loads can be classified into the normal loads and upset loads.

The normal rake loads are a result of viscous stress and pressure forces on surfaces of the rake structures during normal operation, which are induced when the rake rotates at the designated speed and breaks through the yield stress and surrounding mud structure. The normal rake loads are associated with the energy consumption and operational costs for an industry thickener. With evolvement of the gravity thickeners from conventional thickeners characterized by low solids loadings and shallow feedwell configurations (Hazen, 1904), to high-rate thickeners which feature flocculated feed slurry and higher settling rates (McCarty, 1959), paste thickeners of high underflow density (Gollaher, 2010), and deep-cone thickeners with very deep mud beds and steep floors, a clear trend has been seen that the current thickeners tend to produce higher density underflow than the previous ones. Nowadays it is very common that the high-density thickeners produce underflows with yield stress in the range of 30–100 Pa, while the deep cone thickeners generate underflows with yield stresses over 100 Pa (Schoenbrunn, 2011). Both are above what can be achieved in high rate or conventional thickeners, which are typically limited to yield stress from 20 to 30 Pa. Of course, the high underflow density would lead to high normal rake loads for a given thickener since both the viscosity and yield stress of a bed material typically increase with its density, especially when the density exceeds a certain threshold. Therefore, more robust rake structures and associated assemblies are needed for high-density underflow applications.

On the other hand, the rake mechanism can also experience upset loads under some exceptional situations, where significant thick materials may be accumulated in a region on the floor bed as illustrated in Figure 1. If no immediate mitigation action is taken, such an abnormal event would likely cause an operational incident. So, attention should be paid to the upset loads at the rake design stage. The upset loads would be a determinate factor for capacity of the driving system and structure design of the rake system. Although efforts have been made to design the feedwell for an even distribution and the rake mechanism for effective raking action to prevent heavy sediment sloughing on the floor bed, not all the thickeners work at the design condition all the time. Due to fluctuations in the process conditions and variations in feed composition, flocculant dosage, sediment profile, control system, etc., some thick materials may build up unevenly on the floor bed and lead to the drive overloading, rake blockage, or even damage of the rake structure, especially for the paste and deep cone thickeners (Ruan, 2019). Therefore, quantification of the upset load remains a challenge both for thickener designers and operators. It is also the motivation of this study.

To quantify the normal and upset loads on a thickener rake, CFD has demonstrated its effectiveness by numerically integrating the viscous stress and pressure on surfaces of the rake blades and arms in a gravity thickener (Frost et al 1993, Szalai et al. 1994, Šutalo et al. 2003, Rudman, 2008). However, its applications are restricted to the normal rake loads for the lab-scale or pilot-scale

thickeners. The only work for a full-scale industry thickener was presented at 2024 SME annual conference (Lu, et al, 2024). So far, no publication is available for quantification of the upset loads in the open literature. Although it was reported that the rake blockages more frequently occurred in deep cone thickeners for the tailing dewatering application (Ruan 2019), no physical insight and feasible solution were provided to address such the rake-blockage observed.

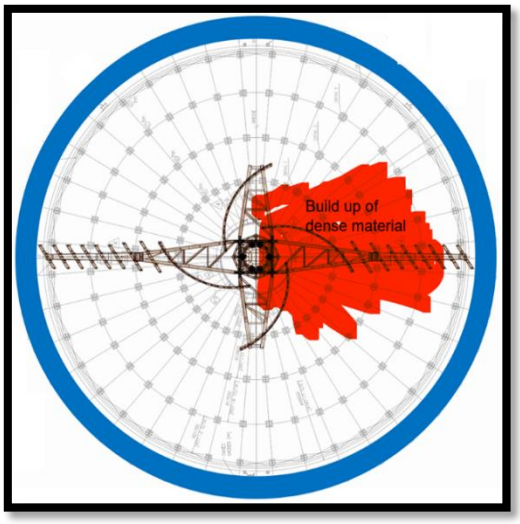

Fig 1 Buildup of thick bed-material

Figure 2 Configuration of FLS raked thickener.

Process Description

Figure 2 shows overall configuration of a raked thickener to be considered in this study, which is an FLS 45m deep-cone thickener (the world's largest DCT) and has the newly patented inner spiral rake blade technology with capability to produce 68wt% underflow on copper tailings. The rake mechanism is composed of four arms with a set of the patented inner spiral rake blades and driven by a hydraulic driving system. The corresponding diameter of the short arms is about 19.5m and the designated rake speed is 0.075RPM. Table 1 lists typical feed condition of this thickener.

Table 1 Typical feed conditions

Feed parameters	**Value**
Solid content (wt%)	31-36
Solid rate (t/h)	1120
Undiluted rate (m^3/h)	2835
Diluted rate (m^3/h)	8613

Assumption 1: To mimic the field observation, it is assumed that some thick material drops to a specific region of the floor bed due to an unexpected cause, thus forms a mud island. Such a mud island could take different shapes. For simplification, a half-sphere is considered with the center right on the inner surface of the floor bed. To capture the worst-case scenario, it is further assumed that all solids carried in the feed stream will contribute to the island formation. With the different raking actions due to the short and long arms, two potential island locations could be formed, which are called the inner island and outer island, respectively.

- **Inner Island**: If all the solid drops in a region within the short-arm periphery (R=9.75m), both short-arm and long-arm could reach and scrape there, the available time interval between the two successive raking actions is about 200s, and an inner island of total volume 33m^{3}will be formed, corresponding to a half sphere of radius 2.5m as shown in Figure 3.
- **Outer Island**: If all the solids were outside of the short-arm's periphery (R=9.75m), the short-arms would not reach the island and only the long-arms can scrape that region. In this scenario, the available time interval between the two raking actions would become 400s, and an outer island of total volume 66.9m^{3}would be formed, corresponding to a half sphere of radius 3.2m as shown in Figure 4

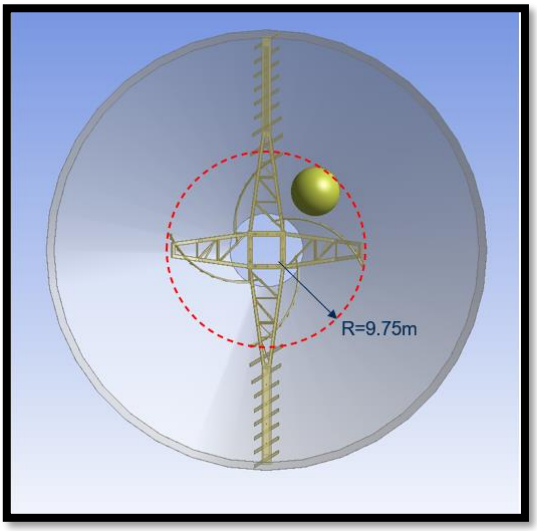

Figure 3 Inner island

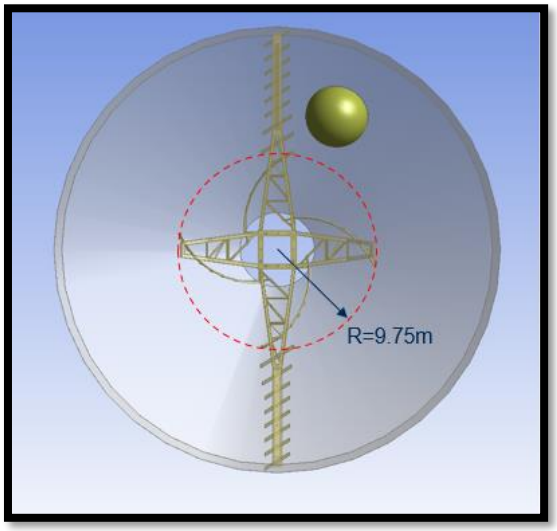

Figure 4 Outer Island

Assumption 2: With lack of material property from a real island formed in field thickener, a semisolid paste with a yield stress of 400Pa shown in Figure 5 is assumed. The rest of thickener tank volume will be filled by the normal mud-bed sediment with the rheology parameters given in Table 2 and flow curves in Figure 5.

Table 2 rheology parameters of Normal sediment & Island materials

Property	**Normal sediment**	**Island material**
Density (kg/m^3)	1765	1950
Yield stress (Pa)	13.85	400
Flow consistency index	0.1	100
Flow behavior index	1	1

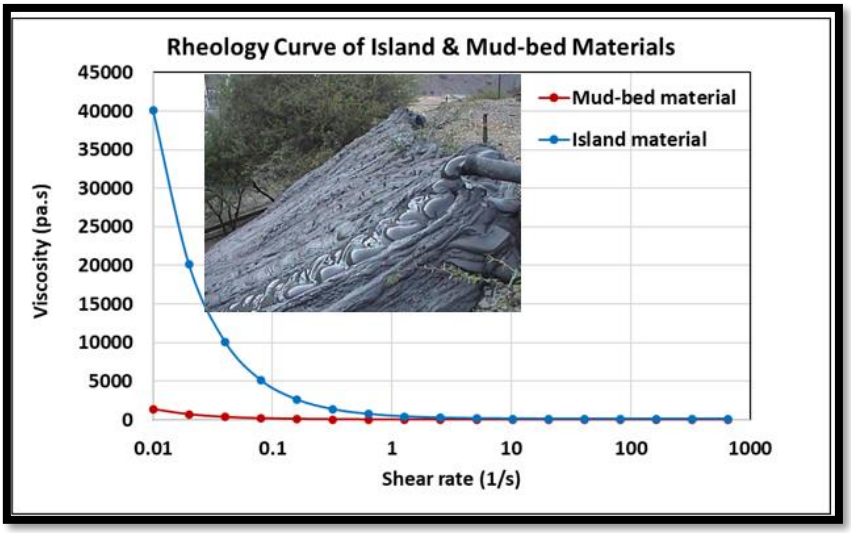

Figure 5 Rheology curves of mud-bed & island materials

Assumption 3: It is further assumed that the rake and associated structures were made of the same materials with mechanical properties given in Table 3

Table 3 Mechanical properties of associated rake structures

Parameter	Value
Elastic modulus	200 GPa
Poisson's Ratio	0.26
Shear modulus	79.3GPa
Density	7850 kg/m^3
Tensile strength	400 MPa
Yield strength	315 MPa

FSI ANALYSIS

In quantification of the rake loads, CFD normally provides the integrated forces (Fx, Fy, Fz) and torques (Tx, Ty, Tz). With these outputs, the question becomes how to effectively apply the CFD solution for a rake design, otherwise, significant uncertainty might be introduced when re-distributing the CFD loads on the rake surfaces for structure design or strength analysis.

To address this question, this paper proposed the one-way FSI approach, where the fluid solution is obtained by Ansys CFD solver, and the structure analysis is carried out by Ansys FEA solver. By coupling the two solvers together, a transient CFD analysis is performed first, the converged solution is then mapped onto the coupled surfaces of FEA model. With such a coupled procedure, all the load transfer and re-distribution are completed at the computational cell scale, and the uncertainties involved in conventional CFD analysis can be eliminated.

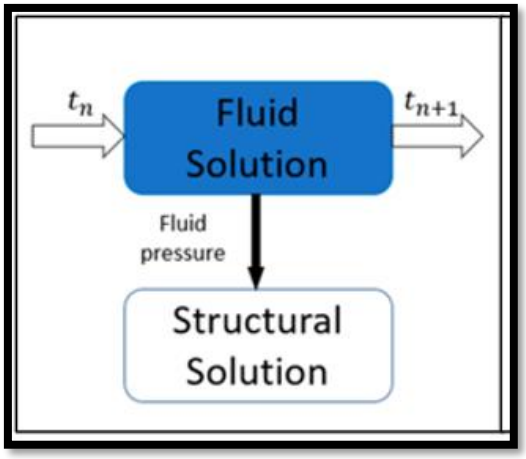

Figure 6 One-way FSI Procedure

CFD Solution

Inner Island: Figure 7 shows the shape change of the inner island before (t=0s) and after (t=200s) the raking action. Due to the double raking actions from the short and long arms, most of the island material is scraped to the underflow region and ready for discharge. Figure 8 compares the predicted profiles of rake torque (Tx, Ty, Tz) and rake force (Fx, Fy, Fz) during the raking process. A significant jump is observed on rotation torque component (Ty). This indicates the rake will withstand a high rotational torque when breaking through the island material, in which a peak value of 240699 N-m occurs at t=80 seconds. Except for the rotational torque (Ty), all other torque and force components remain relatively low or limited response. This reveals that the upset loads due to the inner island would behave largely as a torque spike or sharply increased torque, which agrees well with the field observation.

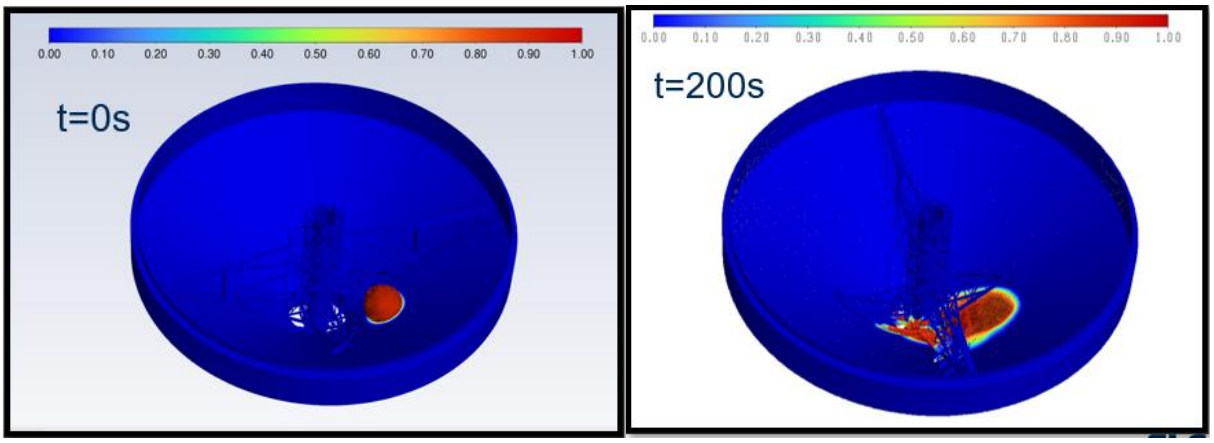

Figure 7 Inner Island shape and location - before and after raking action.

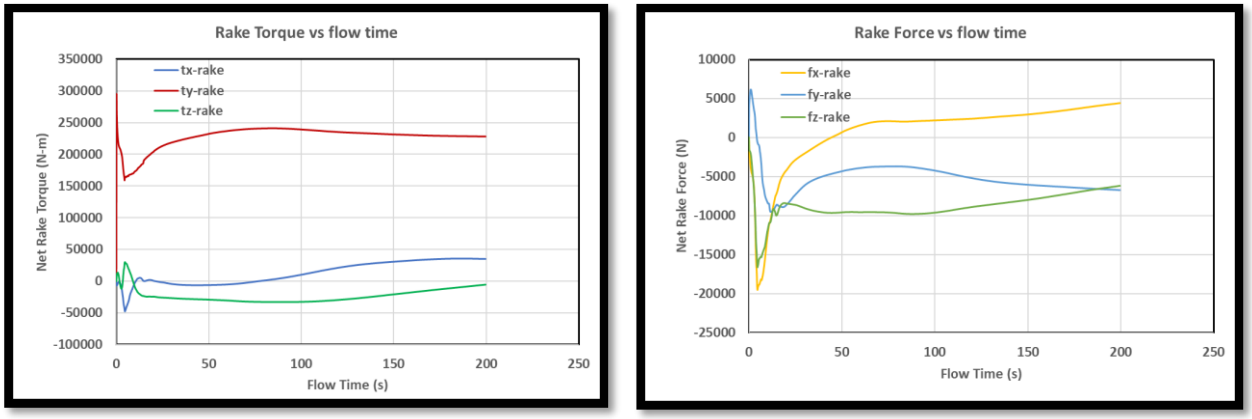

Figure 8 torque and force profile for breaking inner island

Outer island: Similarly, Figure 9 illustrates the shape changes of the outer island before (t=0s) and after (t=200s) the raking action. Since only the long arm can reach the outer island and the single raking action can occur, less island material is scrapped. From the rake torque and force profiles in Figure 10, significant increases are observed in torque Tx and Ty with corresponding peak torque of 366951 N-m at t=40s for Ty, and 180000 N-m at t=150s for Tx. With reference to the inner island scenario, the higher rotational torque of Ty can be attributed to more island materials to be broken and longer distance from the scraping location to rotation center of the rake. The upset load due to the Ty would be a potential cause for the drive overloading, a torque spike, or rake blockage observed in the field. On the other hand, the elevated torque component of Tx as well as the force components of Fx, Fy, Fx indicates that the outer island also induces unbalanced loads that may shift the designated rake position and potentially cause mechanical collision between the rake system and surrounding structures. Therefore, the upset load due to Ty could be a potential cause for drive overloading, while the upset loads due to Tx, Fx, Fy, Fz could be the root-cause of unbalanced loads that lead to mechanical collision, rake blockage, and torque spikes noted in field operation.

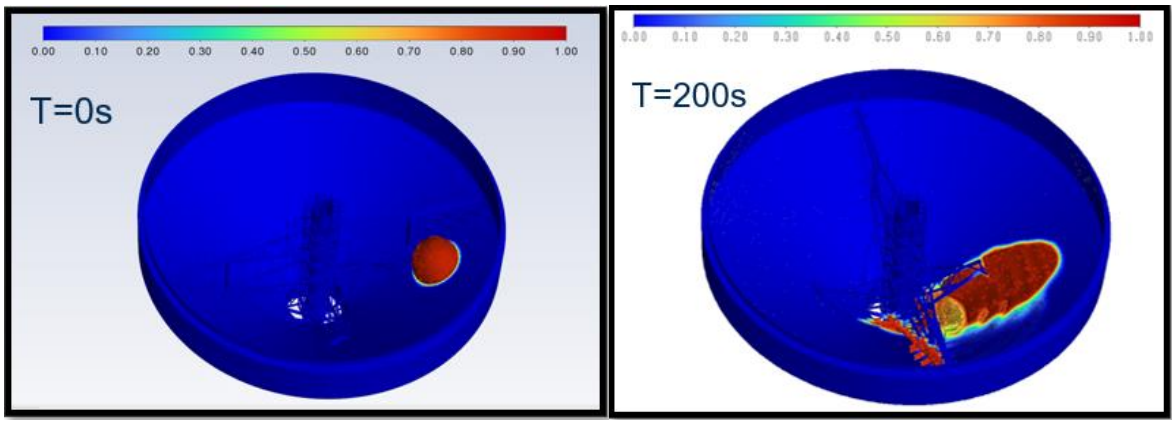

Figure 9 Outer Island shape and location – before and after raking action.

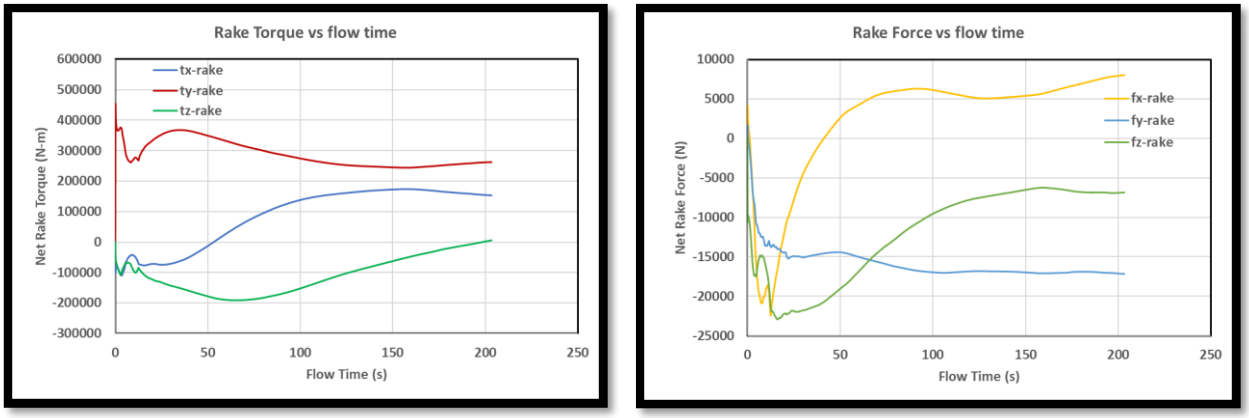

Figure 10 torque and force profiles for breaking outer Island

Comparison: To check relative significance of the upset loads due to island formation, the normal rake load was also predicted, in which the simulation was done under the same conditions except for no presence of any island. Figure 11 illustrates the overall pressure distribution induced by normal mud-bed material, inner island, and outer islands, while Figure 12 compares the normal rake loads against the upset rake loads due to island formation. As can be seen, the inner island would cause 23% more upset torque and 194% higher upset force than those at normal condition, while the outer island leads to 88% more upset torque, and 593% higher upset force, respectively. The high upset torques would be the potential cause for drive overloading, torque spike, etc., while the high upset forces would be the root-cause for torque spike, rake blockage, and other mechanical problem observed in field operation.

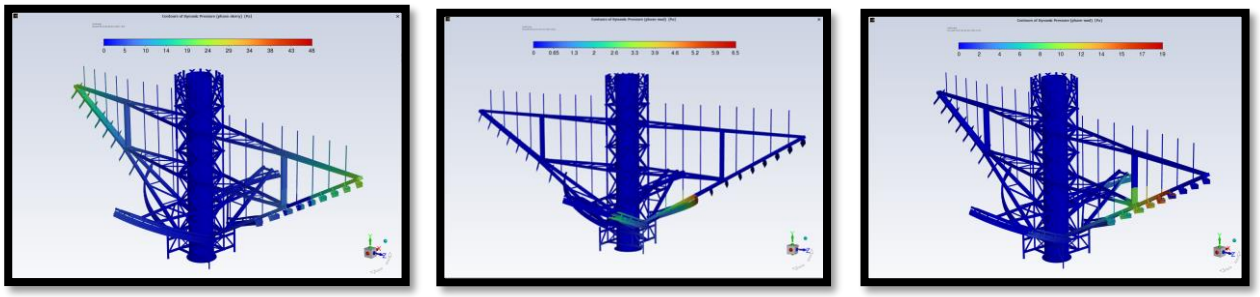

Figure 11 Compared raking pressure – Inner vs outer Island.

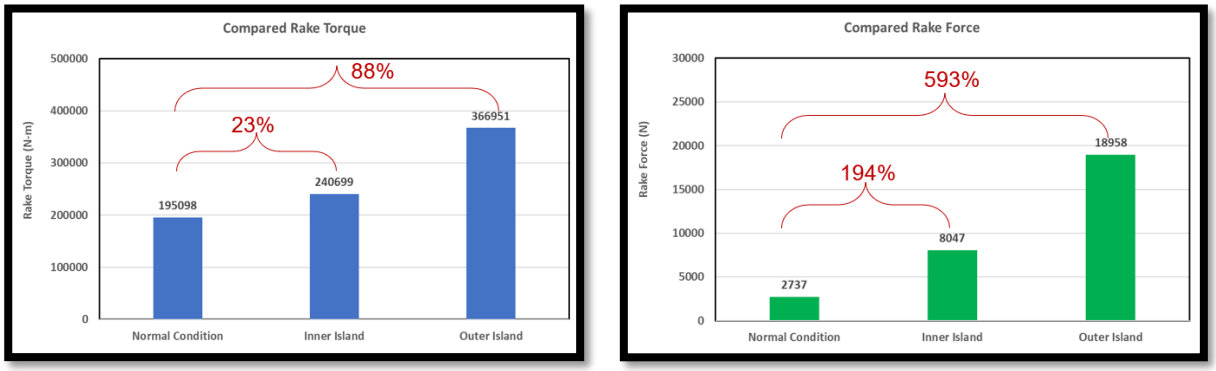

Figure 12 Compared upset loads vs normal loads – Inner vs outer Island

FEA Solution

Inner Island: By mapping the CFD solution onto the coupled surfaces in the FEA model, Figure 13 shows the hydrostatic pressure due to mud-bed slurry and the pressure mapped from CFD due to rake motion, including normal rake load and upset rake loads. The simplified top blocks are added to account for the pre-stress effect due to enclosure and bridge structures. Figure 14 gives the total deformation and stress response from FEA analysis. Both the overall deformation and stress response are at the relatively low levels with peak value of 6.47mm and 65.3Mpa, respectively.

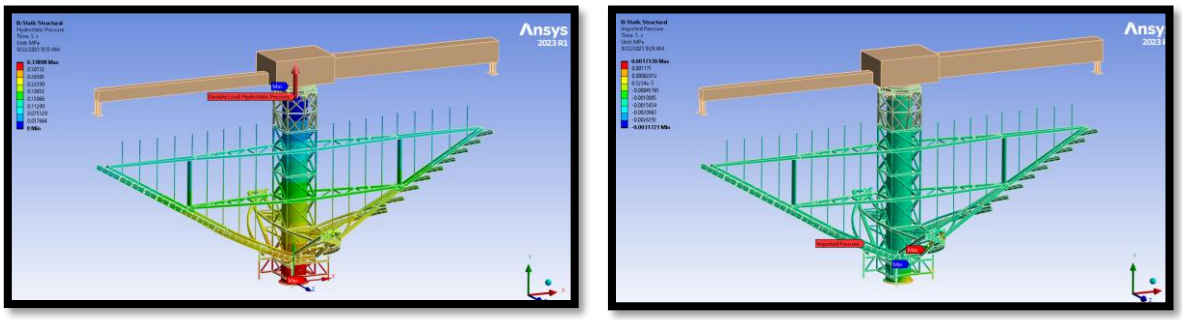

Figure 13 Hydrostatic pressure & pressure mapped from CFD – Inner Island

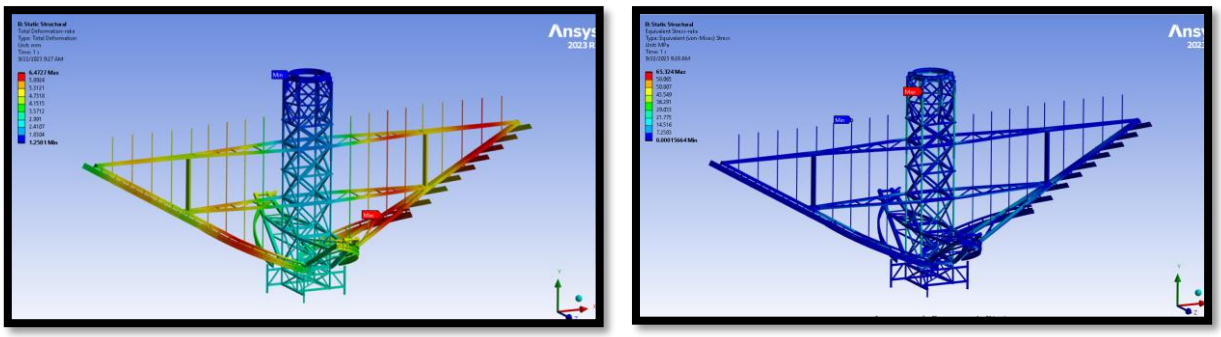

Figure 14 Total deformaiton and stress response – Inner Island

Outer Island: Similarly, Figure 15 presents the hydrostatic pressure, and the mapped pressure loads from CFD solution for the outer island scenario, while Figure 16 shows the corresponding total deformation and stress response from FEA analysis, where a peak deformation of 6.39mm and max stress of 65.7MPa are observed.

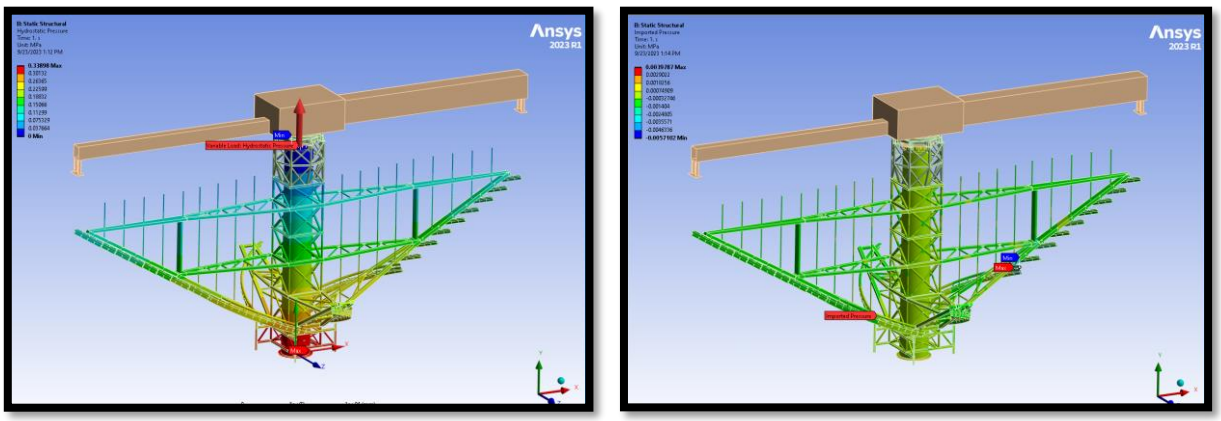

Figure 15 Hydrostatic pressure & pressure mapped from CFD - Outer Isalnd

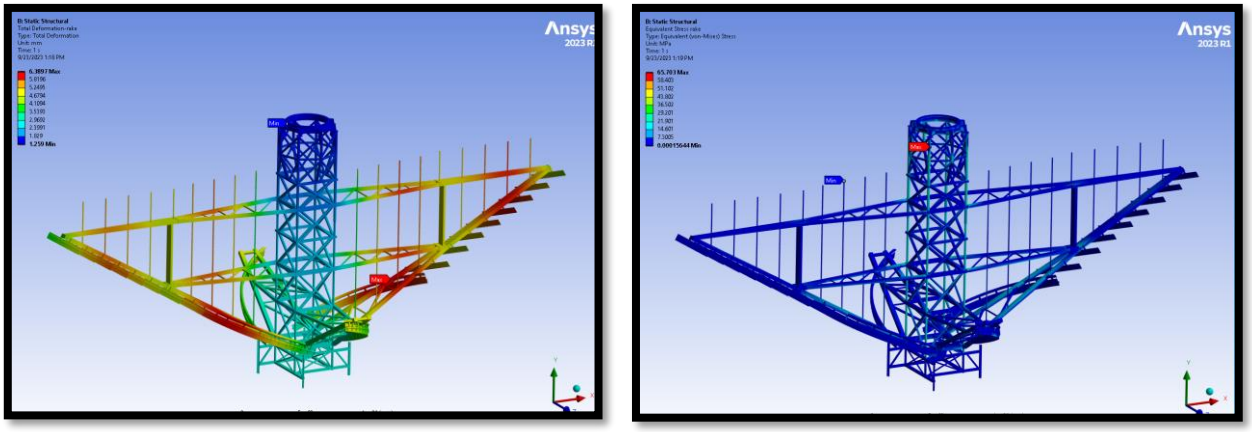

Figure 16 Total deformaiton and stress response - outer Island

Comparison: For comparison purpose, Table 4 summarizes the structure response under action of normal and upset rake loads. With relative to the yield stress of 315MPa given in Table 3, the overall stress of 65MPa is at very low level in both scenarios. This indicates that the upset loads should not be a strength concern for the rake structure. Although Figure 12 shows that formation of the inner and outer islands would cause up to 23% and 88% increase in the rake torque and 194% and 593% jump in rake forces, table 4 doesn't show the consistent outcome on the structure response. This is because the total deformation and max stress given in Table 4 is a combined outcome of the total loads, while the upset loads in Figure 12 are at relatively lower level compared to the other loads or the loads in vertical direction.

Table 4 Structure response to upset loads due to inner and outer islands.

Structure response	**Inner Island t=80s**	**Outer Island t=40s**
Total deformation (mm)	6.47	6.39
Max stress (MPa)	65.3	65.7

Conclusion

- To mimic field observations, two worst-case scenarios of thick material build up in an industry thickener have been investigated, which are the inner island and outer island formation. By applying the FSI approach developed recently, a full-scale and full-physics quantification of the upset loads have been achieved in this study.
- CFD solution reveals that the rake torque reaches its peak value of 240699 N-m at 80 seconds for the inner island, and 366951 N-m at 40 seconds for the outer island, respectively. The outer island induces higher upset loads due to more thick material built up and longer distance from the scrape location to rotation center of the rake. With comparison to the normal rake loads, the inner island would cause 23% more upset torque and 194% more upset force, while the outer island would lead to 88% more upset torque and 593% upset force.
- The upset rotational torque should be an important sizing factor for capacity of the driving system and structure design of the rake system. It could be a potential cause for some operational incidents during the field operation, including the drive overloading, rake-blockage, torque spike, etc., all the nonrotational upset loads (torques and forces) could be the root-cause for unbalance loads that leads unexpected mechanical problems of the rake system.

- The FEA solution shows a total deformation of 6.5mm and peak stress about 65MPa, both of which are at relatively low levels. This indicates that the upset loads have little or limited influence on the structure response and should not be a deciding factor for strength analysis and/or rake structure design. This can also be interpreted that the current rake structure has been adequately designed, while FSI solution provides deep insight for future optimization.
- This study has demonstrated the applicability and effectiveness of FSI approach for quantification of the upset loads in a raked thickener. With further verification on the assumptions, such a high-fidelity approach can be applied for sizing a new thickener or troubleshooting an existing thickener.

References

1. Warden, J.H., The design of rakes for continuous thickeners especially for waterworks coagulant sludges. Filtration Separation. March/April 1981, pp113–116
2. Gunthert, F.W., Thickening zone and sludge removal in circular final settling tanks. Water Science & Technology, 1984 (16), pp303–316.
3. Albertson, O.E., Okey, R.W., Evaluating scraper designs. Water Environment Technology, January 1992, pp52–58.
4. Frost, R.C., Halliday, J., Dee, A.S., Continuous consolidation of sludge in large scale gravity thickeners. Wat. Sci. Technol. 1993 (28), pp77– 86.
5. Rudman, et al, Raking in gravity thickeners, Int. J. Miner. Process. 2008 (86), pp114–130
6. Rudman, M, Paterson, D.A., Simic, K., Efficiency of raking in gravity thickeners, International Journal of Mineral Processing, 2010 (95), pp30–39
7. Sutalo, I.D., Paterson, D.A. Rudman, M, Flow visualization and computational prediction in thickener rake models, Minerals Engineering 2003 (16), pp93–102.
8. Lu, Y.J., Sok, T., Schoenbrunn, F., Scott, J., and Gilbert, C., FSI Analysis of Mud-Rake Interaction in a Full-scaled Thickener, 2024 SME Annular Conference, February 25-28, 2024, Phoenix, AZ
9. Hazen, A, On Sedimentation, Trans ASCE, 1904(53), pp 45-71.
10. McCarty, MF. Olson, R. Polyacrylamides for the Mining Industry, Mining Engineering, Jan 1959, pp 61-5.
11. Gollaher,T, Johnson, JL, Biesinger, MT, Accioly, AHL, Paste Thickening Tailings – Recent Examples of a Rapidly Emerging Technology, SME Annual Meeting 2010
12. Schoenbrunn, F, Dewatering to Higher Densities — An Industry Review, Paste 2011 — R.J. Jewell and A.B. Fourie (eds)
13. Ruan, Z., Wang, Y., Wu, A.X., Yin, S.H., and Jin, F., A Theoretical Model for the Rake Blockage Mitigation in Deep Cone Thickener: A Case Study of Lead-Zinc Mine in China, Mathematical Problems in Engineering Volume 2019, Article ID 2130617.